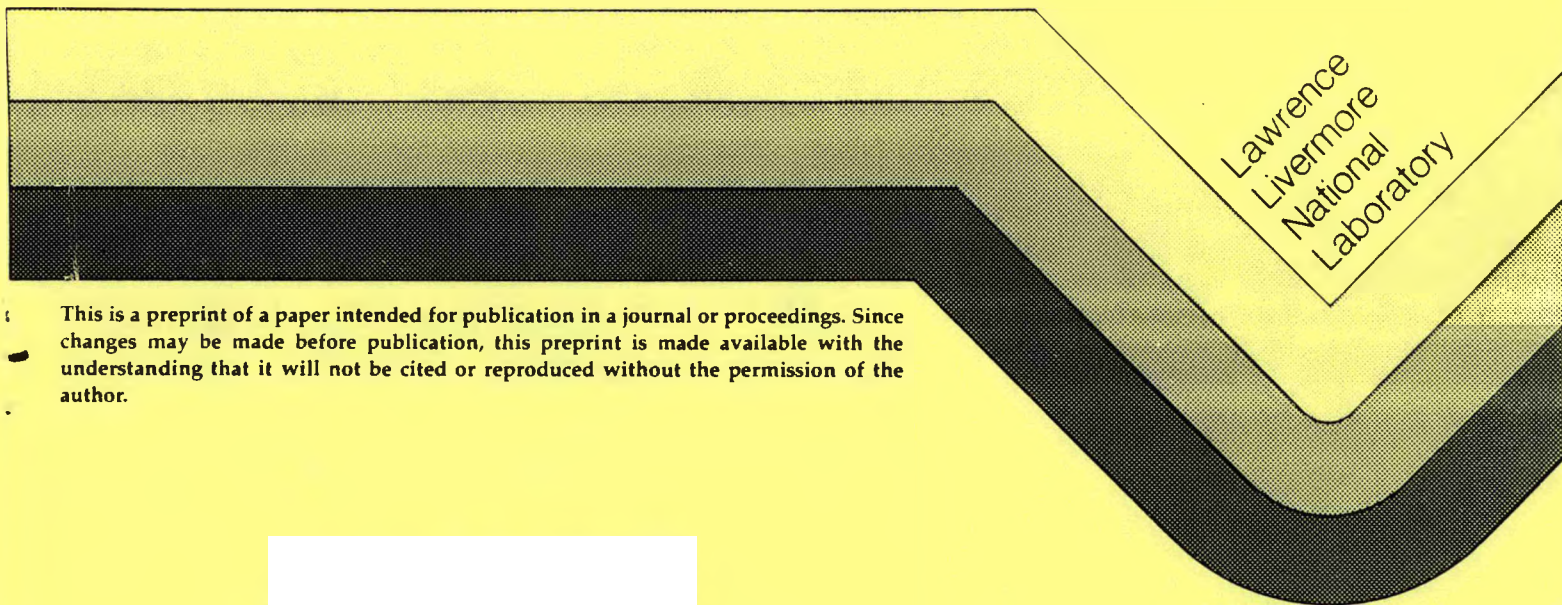


NITROGEN CHEMISTRY DURING OIL SHALE PYROLYSIS

Myongsook S. Oh
Richard W. Crawford
Kenneth G. Foster
Armando Alcaraz

This paper was prepared for submittal to
Eastern Oil Shale Symposium
Lexington, KY
11/15-17/89

January 10, 1990



This is a preprint of a paper intended for publication in a journal or proceedings. Since changes may be made before publication, this preprint is made available with the understanding that it will not be cited or reproduced without the permission of the author.



DISCLAIMER

This report was prepared as an account of work sponsored by an agency of the United States Government. Neither the United States Government nor any agency thereof, nor any of their employees, makes any warranty, express or implied, or assumes any legal liability or responsibility for the accuracy, completeness, or usefulness of any information, apparatus, product, or process disclosed, or represents that its use would not infringe privately owned rights. Reference herein to any specific commercial product, process, or service by trade name, trademark, manufacturer, or otherwise does not necessarily constitute or imply its endorsement, recommendation, or favoring by the United States Government or any agency thereof. The views and opinions of authors expressed herein do not necessarily state or reflect those of the United States Government or any agency thereof.

DISCLAIMER

Portions of this document may be illegible in electronic image products. Images are produced from the best available original document.

NITROGEN CHEMISTRY DURING OIL SHALE PYROLYSIS

Myongsook S. Oh, Richard W. Crawford, Kenneth G. Foster, and Armando Alcaraz
Lawrence Livermore National Laboratory
P.O. Box 808, L-207
Livermore, CA 94550

Abstract

Real time evolution of ammonia (NH_3) and hydrogen cyanide (HCN), two major nitrogen-containing volatiles evolved during oil shale pyrolysis, was measured by means of a mass spectrometer using chemical ionization and by infrared spectroscopy. While the on-line monitoring of NH_3 in oil shale pyrolysis gases was possible by both techniques, HCN measurements were only possible by IR. We studied one Green River Formation oil shale and one New Albany oil shale. The ammonia from the Green River oil shale showed two distinct peaks, while the New Albany shale showed one broad NH_3 peak maximizing at a high temperature. For both oil shales, most NH_3 evolves at temperatures above oil-evolving temperature. The important factors governing ammonia evolution were the presence of inorganic ammonium salts such as Buddingtonite in Green River oil shales, the distribution of nitrogen functional groups in kerogen, and the retorting conditions. The gas phase reactions, such as NH_3 decomposition and HCN conversion reactions, also play an important role in the distribution of nitrogen volatiles, especially at high temperatures. Although pyrolysis studies of model compounds suggests the primary nitrogen product from kerogen pyrolysis to be HCN at high temperatures, we found only a trace amount of HCN at oil-evolving temperatures and none at high temperatures ($T > 600^\circ\text{C}$).

Introduction

The study of nitrogen (N) species released during oil shale processing is an important research area because both oil shale and shale oil are rich in N. Combustion of N-bearing fuels can produce nitrogen oxides (NO_x), and the emissions of NO_x are limited by law due to environmental concerns. Ammonia is a major N by-product in oil shale processing. Ammonia accounts for most of the N in the retort water and pyrolysis gas streams, and a trace amount of HCN was also observed in those product streams.¹ Both

ammonia and HCN are important intermediates in the formation of NO_x during combustion.

We studied NH_3 evolution by pyrolyzing oil shale under a given time-temperature history and measuring the total yield of NH_3 by an ammonia electrode.² We learned that: the NH_3 yield increased rapidly as the final pyrolysis temperature increased above 500°C ; NH_3 evolved at oil-generating temperatures came from organic N, while the high temperature NH_3 was from both organic and inorganic sources; the yield at $T > 500^\circ\text{C}$ was affected by the NH_3 decomposition reaction; and steam worked as an inhibitor for NH_3 decomposition. The ammonia electrode was simple to operate and gave accurate measurements of total ammonia yield for a given pyrolysis condition. However, the electrode method is rather a cumbersome way

¹Current Address: Texaco Inc. Research and Environmental Affairs Department, P.O. Box 509, Beacon, NY 12508

MASTER

to study ammonia evolution kinetics. Earlier, we reported an on-line technique for measuring real-time evolution of NH_3 by means of a mass spectrometer using isobutane chemical ionization.²⁴ In this paper, we summarize the on-line NH_3 evolution rates for one Green River Formation oil shale and one Eastern oil shale as they were pyrolyzed with inert gas (argon) sweep and under autogenous conditions. We also report the evolution of HCN, measured by an infrared spectrometer (IR). We discuss organic/inorganic sources of N and the contribution of the different nitrogen functional groups in kerogen to the NH_3 yield at different pyrolysis temperatures. We also discuss the gas-phase secondary reactions of N volatiles during oil shale pyrolysis.

EXPERIMENTAL

We employed one Green River Formation (western) oil shale and one Eastern U. S. Devonian oil shale in this study. The Green River oil shale was from the Mahogany zone, obtained from Anvil Points mine, CO and has the grade of 22 gal/ton (AP24). The Devonian oil shale was from the New Albany Shale high-grade zone, obtained from Bullitt County, KY, and has the grade of 13 gal/ton (NA13). The chemical compositions of the two oil shales are summarized in Table 1.

About 1 g of oil shale was loaded into a 3/8" o.d. x 21" long quartz tube. We used quartz reactors to minimize reactions with the retort material. We varied the reactor design and the sample size with heating rate to insure the uniform sample temperature during heat-up. The reactor was then placed in a 0.75" i.d. tube furnace. The furnace was heated linearly from 25°C to 900°C. The control thermocouple for the furnace was placed in the inside wall of the furnace. The sample temperature followed the furnace temperature with a roughly constant time lag, unless either endothermic or exothermic reactions occur in the sample bed. In this report, we included the data from pyrolysis at 10 °C/min only. The sweep gas of argon flowed at 40 cm³/min at 25°C. In the case of autogenous retorting, 40 cm³/min of argon was introduced down stream of the retort, just above the oil trap. In all cases, the sweep gas plus volatiles flowed through a glass wool trap placed in a 130°C oven to condense heavy components (oil) and then fed to a triple-quadrupole mass spectrometer (TQMS) via an 1/8" stainless steel transport line,

Table 1. Chemical Compositions of AP24 and NA13, wt %.

	NA13	AP24
Total C	11.9	16.0
Acid CO ₂	1.30	17.8
Org. C	11.5	11.1
Total H	1.48	1.71
Total N	0.43	0.59

heated at 140°C. For ammonia measurements, it is necessary to heat all lines from the reactor to the detector to minimize NH_3 adsorption and desorption as well as ammonia dissolution into condensed water.

The NH_3 concentration in the product gas stream was measured by the TQMS using isobutane chemical ionization (CI).⁴ In the electron impact (EI) mode which is a more common ionization technique, the fragment of H_2O (OH) and some methane (¹³CH₃) interfere with NH_3 at m/z 17. The interference by H_2O is very troublesome for NA13, which is a wet shale and evolves much more H_2O than NH_3 . In the CI mode using isobutane as a CI reagent, NH_3 could be determined in the presence of water as ammonium ion (NH_4^+) at mass 18, because the ionization of water was very inefficient, and almost all the water ions appeared as the protonated species at mass 19. We monitored a few fragments of isobutane and used their profiles to correct the NH_3 evolution profile for long- and short-term TQMS instrumental instabilities. Ammonia evolution profiles were also corrected for the variation of the total flow, and then the calibration factor, which was determined using an 1.08 % or 144 ppm NH_3 standard in argon, was applied.

We tried to introduce a constant flow of trimethylamine or steam at the exit of the oil trap, to monitor the variation of total flow due to volatiles formation. However, neither trimethylamine nor the steam worked well as a flow monitor. The trimethylamine was difficult to handle because of its strong odor and tendency to polymerize and plug the transport line. With steam, it was difficult to establish and maintain a constant flow at a low flow rate (< 100 cm³/min). So we have decided that the best way of getting the total flow information is to run duplicate experiment in EI mode, in which the total flow rate, sweep gas plus total volatiles flow, can be obtained from the profile of the sweep gas.⁵

We determined the calibration factor before and after each retorting experiment. Because ammonia adsorbs on all surfaces it encounters, we had to allow the calibration gas to flow for a long time (30 mins for 1% NH_3 in argon) before it reaches a constant ammonia concentration. During retorting, the calibration gas was kept flowing through an exit vent at a constant rate. This keeps all surfaces saturated for the final NH_3 calibration.

RESULTS

We have run three identical experiments to determine the reproducibility of our on-line technique. We used AP24 and a 10 °C/min heating rate. Figure 1 shows the ammonia evolution profiles as a function of time from the three runs along with a time-temperature history. The profiles are not corrected for the variations in the total flow. As can be seen, the ammonia profiles by the TQMS are very reproducible. The standard deviation of the areas under three profiles was 2.4 %. The sample temperature increases linearly

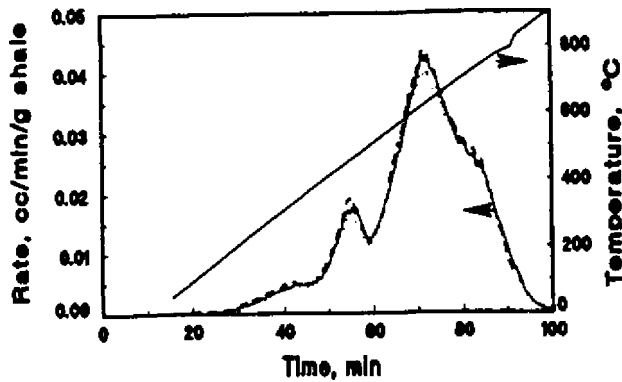


Figure 1. Triplicate measurements of ammonia evolution from AP24 at the 10 °C/min heating rate with time-temperature history.

Table 2. Comparison of ammonia yields ($\mu\text{g NH}_3/\text{g shale}$), measured by a TQMS and by an ammonia electrode.

	NA13	AP24
	<u>By TQMS</u>	
With Sweep		
Integrated to		
550°C	291	224
900°C	772	841
Autogenous		
550°C	171	193
900°C	954	996
	<u>by Electrode</u>	
Peak Temperature (with Sweep)		
- 530°C	272	380
- 737°C	914	853

until it reaches $T = 780^\circ\text{C}$. This deviation from linear heat-up results from the endothermic carbonate decomposition reaction and causes the profile to have an artificial shoulder when it was plotted as a function of temperature as will be shown in Figure 2b.

Figure 2 shows NH_3 evolution profiles from the two oil shales at a heating rate of 10 °C/min. The ammonia evolution profile from AP24 has a shoulder at around 350°C, a peak at around the oil-generating temperatures, and a broad high temperature peak considerably larger than the first peak. The high temperature shoulder at 780°C is caused by the nonlinearity of the temperature as mentioned before. The shoulder at 700°C was caused by the noise in the sweep gas profile which was used for the flow correction. By contrast, NA13 has one major peak, although there seems to be a shoulder at around 450°C. The ammonia peak from NA13 is broader and the temperature at the maximum rate of evolution (T_{max}) is higher for NA13 than the T_{max} of the high temperature peak of AP24. At these high temperatures, ammonia decomposes to form N_2 and H_2 .² Therefore, the different T_{max} may reflect different catalytic potentials of the different oil shale surfaces for the decomposition reaction rather than the difference in the sources and formation mechanisms of NH_3 .

It is useful to compare the ammonia yield by the TQMS with total yields measured by using an NH_3 electrode. Table 2 summarizes the yields of NH_3 integrated up to 550°C and up to 900°C and compares them with those from the electrode method. We chose a slightly higher temperature for the intermediate integration point to compensate for the holding time in PT experiments. As shown, for the experiments under argon, the TQMS gives reproducible yields that compare well with the yields determined by the NH_3 electrode. Table 2 also includes the ammonia yields from autogenous experiments.

Figure 3 compares the rate of NH_3 evolution from sweep gas retorting with that from autogenous retorting for the two oil shales.

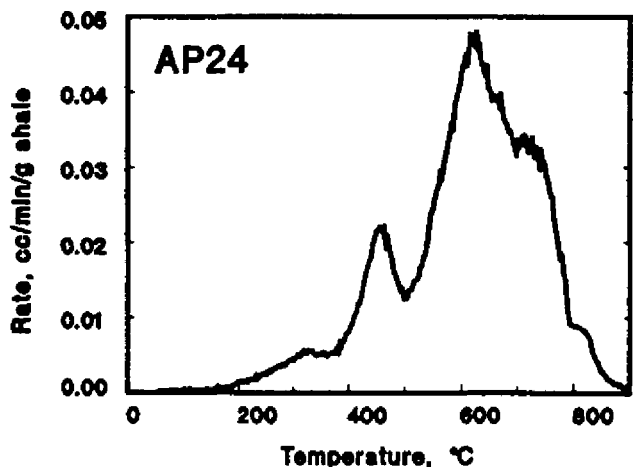
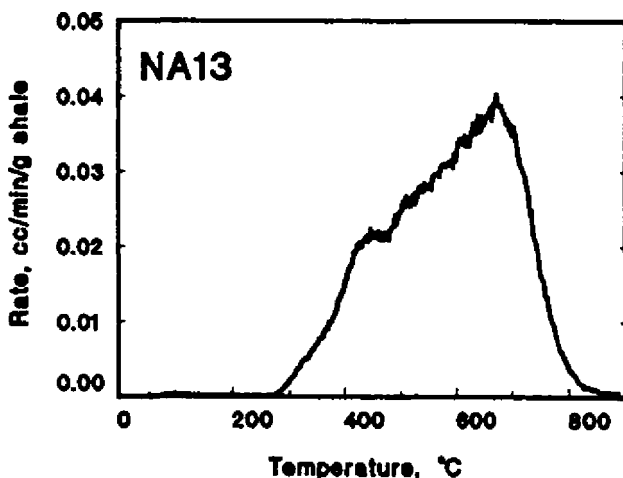


Figure 2. Ammonia evolution from NA13 and AP24.

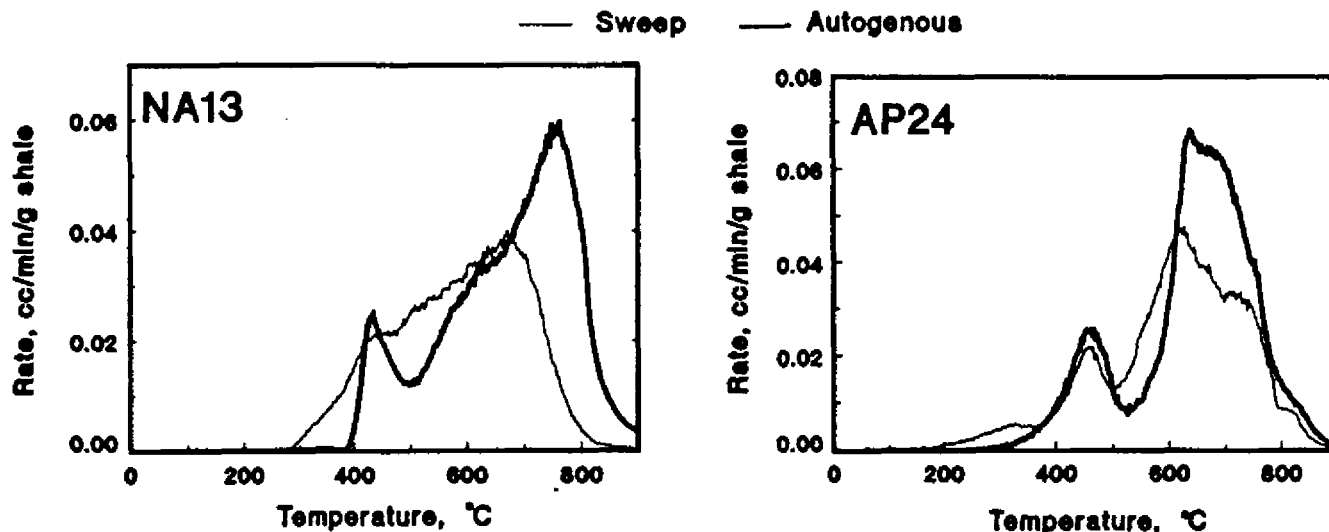


Figure 3. Ammonia evolution from NA13 and AP24 with and without sweep gas.

The AP24 no longer shows the low temperature shoulder under autogenous conditions, and there was much more ammonia evolved at high temperatures. The autogenous retorting of NA13 shows a prominent low temperature ammonia peak and again much higher ammonia yield at high temperatures. For both shales, autogenous retorting gives an ammonia peak with a higher T_{max} .

The on-line measurement of HCN by a TQMS was impossible because m/z 27 is a common fragment of hydrocarbons present in oil shale pyrolysis gas. In addition, the concentration of HCN was low. The other on-line possibility was an IR. We have connected our heated gas transport line to the Digilab FTS-40 FTIR for semi-quantitative measurements of gas evolution. The FTIR was fitted with a special heated light pipe-detector system, normally used for detecting effluent from a gas chromatograph. Even though our FTIR system is not as optimized for on-line data acquisition as the TQMS, we

were able to complete a scan every 6.5°C at $T < 550^\circ\text{C}$ and 32°C at $T > 550^\circ\text{C}$ at 10 °C/min heating rate and plot evolutions of ammonia and HCN as a function of temperature. It was encouraging to see that the ammonia profile duplicates that monitored by the TQMS. Only a trace amount of HCN was observed at low temperatures for AP24 as shown in Figure 4, and no detectable amount of HCN was seen in the case of NA13.

Discussion

In order to understand the chemistry involved in NH_3 evolution, we need to look into the distribution of organic/inorganic N sources in oil shales, N functional groups in kerogen, and the extent of NH_3 decomposition reaction over retorting oil shale surfaces under pyrolysis gas environment.

AP24 contains an inorganic N source, Buddingtonite which is an ammonium-containing feldspar.⁶ Buddingtonite starts to decompose at around 400°C at the 10 °C/min heating rate, and it is a source of at least half of the NH_3 evolved at high temperatures.^{2,3,7} The NH_3 evolution profile from NA13, in which no detectable amount of Buddingtonite was found, suggests that a large amount of NH_3 can evolve from the char matrix at high temperatures. In addition, NA13 is a char-prone oil shale; Fischer assays of this oil shale produce char which contains 55 % of the original organic carbon compared to 20 % from Green River oil shales. Therefore, we expect that NA13 would generate a larger amount of NH_3 from char than Green River oil shales.

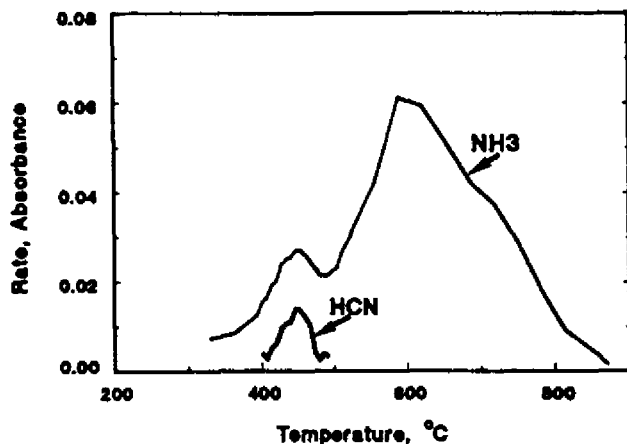


Figure 4. Evolution of NH_3 and HCN from AP24 measured by an FTIR.

While all hydrocarbon gases from oil shale pyrolysis, except CH_4 , evolve at around oil-evolving temperatures (between 400 and 600°C at the 10 °C/min heating rate), the higher evolution temperature for most NH_3 from organic N seems to be related to the N-functional types in kerogen and their pyrolysis chemistry. The principal N-

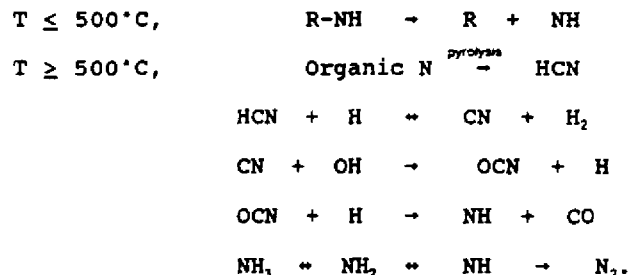
containing species in oil shale kerogen are pyrrole and pyridine types, and there are also some aliphatic N, such as nitriles and amides.⁶⁻¹⁰ Pyrolysis of model compounds of pyrroles and pyridines at low temperatures (roughly $T < 750$ °C) produced mostly rearrangement products and some hydrocarbon gases, but no N-containing species as a gaseous product.^{11,14} At higher temperatures, the rupture of the C-N bond in a ring structure produces HCN, NH₃, and N₂.¹⁵⁻¹⁹ The rate of pyrolysis of model compounds reported by Axworthy et al.¹⁷ predicts a T_{max} at a heating rate of 4 °C/min, which is similar to the T_{max} of NH₃ from oil shales under steam.³

In contrast, the N in alkyl chains decomposes at lower temperatures even though the literature data were scarce. Polyacrylonitrile decomposes between 250 and 350 °C and gives off NH₃ and HCN as the main volatile products. The decomposition of Nylon-66, which breaks the -NH-CO- link, has a much lower activation energy (15 - 42 Kcal/mol) than ring compounds.²⁰ So it is probable that while the low temperature NH₃ comes from N in alkyl chains, the high temperature NH₃ can come from the pyrolysis of heterocyclic ring compounds, and that the distribution of alkyl and aromatic N can also cause the bimodal evolution profile. The high pyrolysis temperature of pyrroles and pyridines also cause the char produced at 500 °C to have a higher organic N/organic C ratio than that in raw shale.^{3,21,22}

The model compound pyrolysis also suggests that the primary pyrolysis product from N in

oil shale char should be HCN, not NH₃, as we observed in Figure 4. For example, Patterson et al.¹⁵ reported that the pyrolysis of pyrrole produced HCN in 49 % yield, and Axworthy et al.¹⁷ observed that the pyrolysis of pyridine yielded 40 % of the N as HCN with an upper limit of 5 % as NH₃ at 960 °C. However, the composition of N volatiles from fuel pyrolysis seems to depend on pyrolysis conditions. For example, industrial coking of coal yields N mainly as NH₃ and N₂, due to NH₃ decomposition.²¹ A high degree of conversion of coal-N to HCN gas was observed under very high heating rate conditions, while most gasifier N exist as NH₃.²² In our fluidized-bed recycle retort system with AP24, the pyrolysis gas contained eight times more NH₃ than HCN at 500 °C,² and the combustor gas at 625 °C contained only a trace amount of HCN, while there was twice as much NH₃ as NO.²⁴ Therefore, it is clear that the secondary reactions of N volatiles in gas phase play an important role in N product distribution.

The NH₃ formation mechanism from kerogen can be summarized as follows:²²



The mechanism of converting HCN to NH₃ and OH implies the possibility of hydrolysis reaction with HCN. We tested the above mechanism by flowing argon with 1% HCN through a retort filled with quartz sand at a rate of 40 cm³/min. The TQMS monitored HCN concentration as well as product gases. The same experiment was repeated with argon with 0.5% HCN and 1.18% H₂O. Figure 5a plots the HCN concentration in the exit stream with and without water vapor, and Figure 5b plots NH₃ produced from HCN. Only 10% of the HCN was decomposed at 900 °C without H₂O, while almost 40% of the HCN is converted in the case with H₂O. No significant amount of ammonia is observed when there is no steam present and, with steam, roughly 60% of the HCN loss is seen as NH₃. This observation supports the above mechanism, and further emphasizes the importance of gas phase secondary reactions in N-volatile product distribution. In addition, it is quite probable to have a 100% conversion of HCN under our retorting conditions, in which the ratio of N volatiles to H₂O is roughly 1 to 20.

Comparison of NH₃ evolution profiles with and without sweep gas shows the effect of both gas-solid and gas phase secondary reactions. Under autogenous conditions, the residence time of volatiles increases as well as the partial pressure of volatiles. As a result, both gas-solid and gas phase secondary reactions are enhanced. The longer residence time of volatiles may have caused the

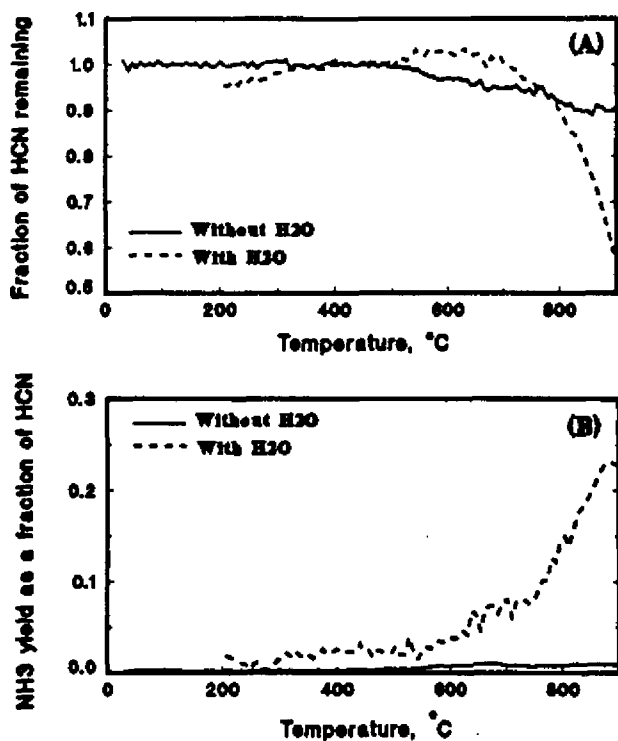


Figure 5. HCN hydrolysis reactions. (A) HCN decomposition; (B) NH₃ from HCN.

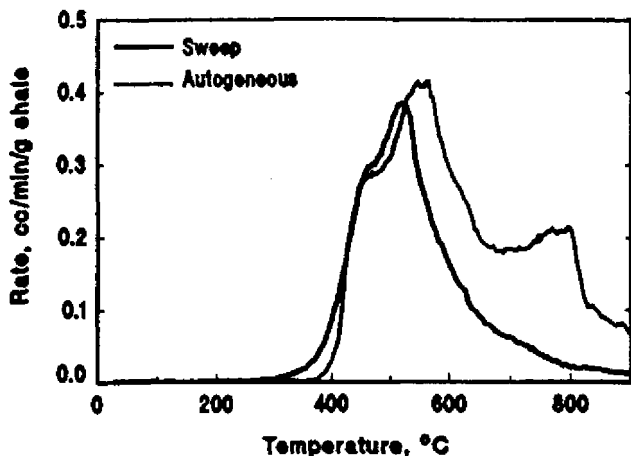


Figure 6. Methane evolution from NA13 and AP24 with and without sweep gas.

disappearance of the low temperature shoulder for AP24 and the sharper ammonia peak at around oil-evolving temperature. The effect of oil cracking does not seem to be important. The ammonia yields up to $T = 550^{\circ}\text{C}$ were about the same in both sweep and autogenous experiments. At high temperatures, higher partial pressure of H_2O and CO_2 and longer residence time enhance char gasification reactions which releases more C as well as N from char. We have observed that much more methane is produced from char gasification at autogenous conditions as shown in Figure 6. The higher partial pressures of H_2O and H_2 also suppress NH_3 decomposition reactions and promote HCN conversion to NH_3 .

Conclusions

We measured the real-time evolution of NH_3 and HCN from one Green River formation oil shale and one Eastern U.S. Devonian oil shale. The NH_3 from the Green River Formation oil shale has two distinct peaks, while the New Albany oil shale has one broad peak maximizing at a high temperature. The high temperature peak is due to NH_3 from the decomposition of hetero-cyclic organic N-compounds and, for AP24, the contribution of inorganic N, Buddingtonite, is also significant. We found only a trace amount of HCN at oil-evolving temperatures and none at high temperatures. The gas phase reactions, such as NH_3 decomposition and HCN hydrolysis, play an important role in N-volatile product distribution at high temperatures for both oil shales.

References

1. Sklarew, D. S., and Hayes, D. J., "Trace Nitrogen-Containing species in the Off Gas from Two Oil Shale Retorting Processes," *Env. Sci. Tech.*, **18**(8), 600-603 (1984).
2. Oh, M. S., Taylor, R. W., Coburn, T. T., and Crawford, R. W., "Ammonia Evolution

during Oil Shale Pyrolysis," *Energy Fuel*, **2**(1), 100-105 (1988).

3. Oh, M. S., Crawford, R. W., Foster, K. G., and Alcaraz, A., "Ammonia Evolution from Western and Eastern Oil Shales," *Prepr. Pap. -Am. Chem. Soc., Div. Pet. Chem.* **34**(1), 94-102 (1988).
4. Crawford, R. W., Coburn, T. T., Miller, P. E., and Oh, M. S., "On-line, Mass Spectrometric Determination of Ammonia from Oil Shale Pyrolysis using Isobutane Chemical Ionization," *Amer. Soc. for Testing and Materials*, STP1019, 133-143 (1989).
5. Oh, M. S., Coburn, T. T., Crawford, R. W., and Burnham, A. K., "Study of Gas Evolution during Oil Shale Pyrolysis by TQMS," *In Proc. Intl. Conf. on Oil Shale and Shale Oil*; Zhu Yajie, Ed.; Chemical Industry Press, Beijing, 1988, 295-302.
6. Taylor, R. W., Burnham, A. K., Smith, G. S., Sanborn, R. H., and Gregory, L. S., "Inorganic Nitrogen in Green River Formation Oil Shale," *Prepr. Pap.-Am. Chem. Soc., Div. Fuel Chem.* **30**(3), 338-348 (1985).
7. Oh, M. S., Foster, K. G., Crawford, R. W., Taylor, R. W., Coburn, T. T., *Thermal Decomposition of Buddingtonite*, Lawrence Livermore National Laboratory UCRL-102156 (1989).
8. Poulsen, R. E., "Nitrogen and Sulfur in Raw and Refined Shale Oils," *Prepr. Pap.-Am. Chem. Soc., Div. Fuel Chem.*, **20**(2), 183-197 (1975).
9. McKay, J. F. and Blanche, M. S., "Analysis of Organic Material Difficult to Recover From Oil Shale," *Liq. Fuels Tech.*, **3**(4), 489-521 (1985).
10. Scouten, C. G., Siskin, M., Rose, K. D., Aczel, T., Colgrove, S. G., and Pabst, Jr. R. E., "Detailed Structural Characterization of the Organic Material in Rundle Ramsay Crossing oil Shale," *Proc. 4th Australian Workshop on Oil Shale*, Brisbane, Dec. 3-4, 1987, 94-100.
11. Patterson, J. M. and Drenchko, P., "Pyrolysis of N-Methylpyrrole and 2-Methylpyrrole," *J. Org. Chem.*, **25**(5), 1950-2 (1962).
12. Jacobson, Jr., I. A. and Jensen, H. B. *Thermal Reactions of Shale-Oil Components: Methylpyrroles, Butylpyrroles, and Isopropylpyrroles*. [Washington] U. S. Dept. of the Interior, Bureau of Mines, 1966.
13. Patterson, J. M. and Soedigdo, S., "Pyrolysis Products of Cycloalkane[a]pyrroles," *J. Org. Chem.*, **32**(10), 2969-71 (1967).
14. Patterson, J. M. and Soedigdo, S., "The Thermal Isomerization of Some Trisubstituted Pyrroles," *J. Org. Chem.*

33(5), 2057-61 (1968).

15. Patterson, J. M., Tsamasfyros, A. and Smith, Jr. W. T., "Pyrolysis of Pyrrolle," J. Heterocyclic Chem. 5(5), 727-9(1968).
16. Cullis, C. F. and Norris, A. C., "The Pyrolysis of Organic Compounds under Conditions of Carbon Formation," Carbon 10, 525-37 (1972).
17. Axworthy, A. E., Dayan, V. H., and Martin, G. B., "Reactions of Fuel-Nitrogen Compounds under Conditions of Inert Pyrolysis," Fuel 57, 29-35 (1978).
18. Houser, T. J., McCarville, M. E., and Biftu T., "Kinetics of Thermal Decomposition of Pyridine in a Flow System," Int. J. Chem. Kinetics 12, 555-568 (1980).
19. Leidreiter, H. I. and Wagner, H. G., "Investigation about the Thermal Decomposition of Pyridine between 1700 and 2000 K," Z. Phys. Chem. (Munich) 153(1-2), 99-108 (1987).
20. Bamford C. H. and Tipper, C. F. H., Chemical Kinetics, Elsevier Scientific Pub. Co., New York, New York, 1975.
21. Campbell, J. H., Gallegos, G., and Gregg, M., "Gas Evolution during Oil Shale Pyrolysis. 2. Kinetic and Stoichiometric Analysis," Fuel 59, 727 (1980).
22. Huss, E. G. and Burnham, A. K., "Gas Evolution during Pyrolysis of Various Colorado Oil shales," Fuel 61, 1188-1196 (1981).
21. Hill, W. H., "Recovery of Ammonia, Cyanogen, Pyridine, and Other Nitrogenous Compounds from Industrial Gases," Chemistry of Coal Utilization, H. H. Lowry Ed., John Wiley & Sons, New York, 1948.
22. Malte, P. C., and Rees, D. P., "Mechanisms and Kinetics of Pollutant Formation during Reaction of Pulverized Coal," Pulverized-Coal Combustion and Gasification, Edited by L. D. Smoot and D. T. Pratt, Plenum Press, New York, 1979.
23. Taylor, R. W. and Morris, C., Internal Memo, LLNL, April 10, 1984.
24. Taylor, R. W. and Morris, C., Internal Memo, LLNL, May 10, 1984.

Acknowledgements

This work was performed under the auspices of the U.S. Department of Energy by the Lawrence Livermore National Laboratory under Contract No. W-7405-Eng-48. Authors also acknowledge Texaco, Inc for the support of M. S. Oh for the preparation of this document.